MDPI

Article

Copper Slag of Pyroxene Composition as a Partial Replacement of Natural Aggregate for Concrete Production

Sandra Filipović [1,*], Olivera Đokić [2], Aleksandar Radević [3] and Dimitrije Zakić [3]

1   Mining and Metallurgy Institute Bor, 19210 Bor, Serbia
2   Highway Institute Belgrade, 11010 Belgrade, Serbia; o.djokic@highway.rs
3   Faculty of Civil Engineering, The University of Belgrade, 11000 Belgrade, Serbia;
    aradevic@grf.bg.ac.rs (A.R.); dimmy@imk.grf.bg.ac.rs (D.Z.)
*   Correspondence: sandra.filipovic@irmbor.co.rs; Tel.: +381-(64)2916545

Abstract: Copper slag, a by-product of the pyrometallurgical process used for obtaining copper from copper ore in Bor, Serbia, contains mainly silicon, iron, calcium, and aluminium oxides. Due to such properties, it is disposed of in landfills. Despite the favourable technical properties copper slag aggregates possess, such as low-water absorption (WA_{24} 0.6%), low resistance to fragmentation (LA 10%), and low resistance to wear (M_{DE} 4%), its use in the construction industry is still limited. The results of testing the technical properties of copper slag aggregates (CSAs) as a potential replacement for natural river aggregate (RA) are presented in this paper. The experiments included tests on three concrete mixtures with partial replacement of coarse natural aggregate with copper slag. The replacement of RA particle sizes of 8/16 mm and 16/31.5 mm with CSA in the amount of 20% + 50% and 50% + 50% resulted in an increase in the compressive strength of 12.4% and 10.5%, respectively. The increase of CSA content led to a decrease in water penetration resistance and salt-frost resistance of concrete, whereas the resistance to chloride ion penetration did not change significantly.

1. Introduction

The global use of about 25×10^9 metric tons per year makes concrete one of the most commonly used construction materials [1]. The possibility of combining with different aggregates in different ratios, wide availability, and economic cost of production established the dominance of concrete in the construction industry [2]. Concrete is widely used in building, bridge, and highway construction and the production of precast concrete elements such as curbs, slabs, pipes, drain channels, etc. The aggregate constitutes up to 80% of the total volume of concrete [3]. Natural aggregates are obtained by crushing rock masses in quarries or extracting sand and gravel from riverbeds. Due to the development of infrastructure in developed and developing countries, there is a huge demand for aggregates, mostly fine aggregates with a high share in the concrete mixture. Active extraction of aggregate deposits from riverbeds can cause serious environmental problems (bed degradation, bank erosion, loss of vegetation, etc.) [4]. The growing need that exists in the construction industry cannot be fulfilled by the available resources. For example, the current river aggregate extraction rate can satisfy only 9% of the total annual demand in China [5]. However, different industrial activities accompanied by the production of primary products result in various by-products that have almost no practical industrial application. These industrial by-products, which are generated in high quantities worldwide, present severe challenges regarding their disposal [6]. This is why it is necessary to find other alternatives that would be acceptable from the ecological aspect. One solution would be the use of copper slag aggregates as a substitute for natural aggregate in concrete [7].

Considering that for each metric ton of produced copper in the world, about 2.2 t of copper slag is generated, almost 24.6×10^6 t of copper slag is generated every year that is disposed of in landfills as waste [8]. Copper slag was thought to be an extremely dangerous material for the environment in the past. This is why the United States Environmental Protection Agency (USEPA) passed a law in 1991 that qualified about 20 waste mineral substances, such as copper slag, as a waste material harmful to the environment [9,10]. In 1996, the UN Basel Convention on the Control of Transboundary Movements of Hazardous Wastes and their Disposal described copper slag as a non-hazardous material, based on which its use was not seen as a threat to the environment [9,10]. Due to the fact that copper slag is composed of non-hazardous chemical materials, its application as a raw material in various industries has been enabled [10].

Copper slag obtained during the first phase of the pyrometallurgical production of copper by oxidizing melting in the blast furnace is an essential recyclable raw material that, in addition to copper (content < 1%), can also contain Zn, Ni, Co, Mo, Sn, and other chemical elements. Further processing of copper slag protects the environment, land, and mineral resources and offers economic benefits. Oxidizing melting of copper concentrate at high temperatures (1200 °C) with the addition of flux (SiO_2) forms copper matte and silicate slag, which floats to the surface due to its lower density (high melting phase) compared to copper matte. After it floats to the surface, it is removed from the smelting system. Part of the iron sulphide oxidizes and reacts with SiO_2, thus producing liquid copper slag with the ferro-silicate matrix as a base, i.e., fayalite (Fe_2SiO_4), while a certain amount is oxidized to magnetite (Fe_3O_4) [11]. While pouring, the hot copper slag is transformed into a solid dark grey mass by abruptly going through the cooling phase and instantaneous crystallization. Due to the drastic temperature change, different-sized granular and incoherent material is formed. Based on the structure, copper slag's quality depends on several factors: type and quality of the raw material used in the smelting process, smelting method, and cooling and rapid crystallization method. As a result, copper slag of different chemical and granulometric composition is obtained [12]. The percentage of different chemical elements in copper slag also depends on the hot copper slag's cooling method at the waste dump [13].

Ravindra et al. [14] investigated the geotechnical properties of copper slag. It was determined that copper slag was a non-plastic material with higher compressibility than sand. The angle of internal friction of copper slag is similar to sand, and its use as backfill behind supporting structures reduces the active lateral resistance. Copper slag is also suitable for use in construction as fill material. Because it does not have any harmful impact on the environment, it can be added to the soil as a material with adequate bearing capacity for road or railway construction or as an aggregate base layer for building foundations.

The investigated physical and chemical properties of copper slag allow it to be used in concrete production as a successful substitute for common aggregates. Due to high particle density, it is suitable for application in mass concrete, concrete slab foundations, or material for the construction of rigid pavement layers [15,16]. By replacing natural aggregate with copper slag aggregate, some concrete properties can be improved, such as compressive strength, density, workability, durability, and flexural strength [17]. M. Khanzadi and A. Behnood [18] showed that the complete replacement of coarse natural aggregate with copper slag increased compressive and tensile strength by 11% and 12%, respectively. The increase of the replacement percentage of natural aggregate with copper slag gradually increased concrete density [19]. Recently, copper slag has been used as a replacement for cement, e.g., in the production of cement clinker [20,21], and as a substitute for fine and coarse aggregate fractions in concrete mixtures and mortar [22]. Copper slag has been tested as a pozzolanic replacement for cement because 70% of the total amount of copper slag in the world contains a favourable combination of SiO_2 + Al_2O_3 + Fe_2O_3 [16]. Due to its pozzolanic activity, it can be used as a cement additive [23]. Depending on the slag's granulated state at the landfill and due to its large specific surface (approximately

400 m^2/kg), the process of grinding and crushing of copper slag requires a high level of energy consumption [13].

As a part of experimental investigation and durability studies [24], tests on resistance to chloride penetration of concrete with partial replacement of natural aggregate with copper slag aggregate were performed. Depending on the method of addition and percentage of copper slag in concrete, the obtained ASTM C1202 results showed that the degree of chloride ingress in concrete with partial replacement of river aggregate with copper slag aggregate was "moderate" or "very low". Concrete formed by adding copper slag as a substitute for natural aggregate is water-permeable, which provides the advantage of use in sidewalks for collecting atmospheric water in cities. Research showed that 100% volume replacement of dolomite with copper slag aggregate in permeable concrete increased the porosity by 3% compared to the control mixture. It can be concluded that the increase of the replacement percentage of dolomite aggregate with copper slag aggregate led to an increase of pore-size distribution in the system, which was further reflected in the increase of water absorption in concrete [25]. This increase seemed to be related to the shape and glassy appearance of the copper slag aggregate's grain surface. Therefore, the porosity of the control concrete samples differed from concrete samples that contained copper slag. Another study showed that water-penetration resistance depended on the pore-size distribution present in the concrete [26]. The shape of the aggregate grains had no significant effect on the freeze-thaw resistance of concrete. However, the content of coarse fractions of aggregate in the concrete determined the frost resistance. The analysis of the obtained results showed a significant relationship between the density of coarse fraction in concrete, water absorption, frost resistance, and durability of concrete [27]. The higher the capillary pores' density and size, the lower the frost resistance [28]. The porosity of concrete mainly depends on the aggregate's grain size, shape, and fraction percentage in the mixture. It was noticed that when the percentage of copper slag in the aggregate mixture was increased, the porosity of concrete increased as well [29,30].

As a manufactured aggregate of the pyrometallurgical process of copper production in Bor, Serbia, copper slag potentially can be used in concrete production. Previous studies performed on this slag confirmed good technical properties [31,32]; however, technical regulations in Serbia viewed copper slag as waste until recently [33,34]. The adjustment following the regulations from the European Union offered the possibility of using copper slag from landfills as a construction material. Therefore, the research presented in this paper is aimed at considering the possibility of using copper slag as an aggregate in concrete. The technical properties of natural aggregate, copper slag aggregate, and concrete mixtures (prepared with partial replacement of natural aggregate with copper slag that had 8/16 and 16/31.5 mm particle sizes) were examined in this paper. Frost resistance, as well as the resistance of concrete to chloride ion penetration, were tested on concrete mixtures made with partial replacement of natural aggregate with copper slag aggregate in order to check the durability of concrete, which has been insufficiently investigated so far.

2. Materials and Methods

Copper slag used in the study was produced by industrial processing in the flotation plant of RTB Bor (Serbia). It was deposited near the processing facilities. The copper slag at the landfill was formed by the process of abrupt cooling of hot copper slag. As the input for the technological process of primary crushing, copper slag grains with sizes up to 600 mm were used, and the output product was loose material with grain size 0–100 mm. The application of these coarse grains could be possible only after further crushing and grinding. Due to economic reasons, for utilizing copper slag in the production of concrete, only aggregate fractions of 8/16 mm (III) and 16/31.5 mm (IV) were used in the research. This decision was based on the initial sample's particle-size distribution curve, which showed that 70% of grains with such size were present at the landfill. Copper slag occurred at the landfill in the form of grains of different sizes that were grey-ochre-purple on the surface (Figure 1a). The samples of copper slag aggregate at the landfill are shown in

Figure 1b. The samples of copper slag aggregate (CSA) used for testing were sieved and then separated into fractions of 8/16 (Figure 1c) and 16/31.5 mm (Figure 1d).
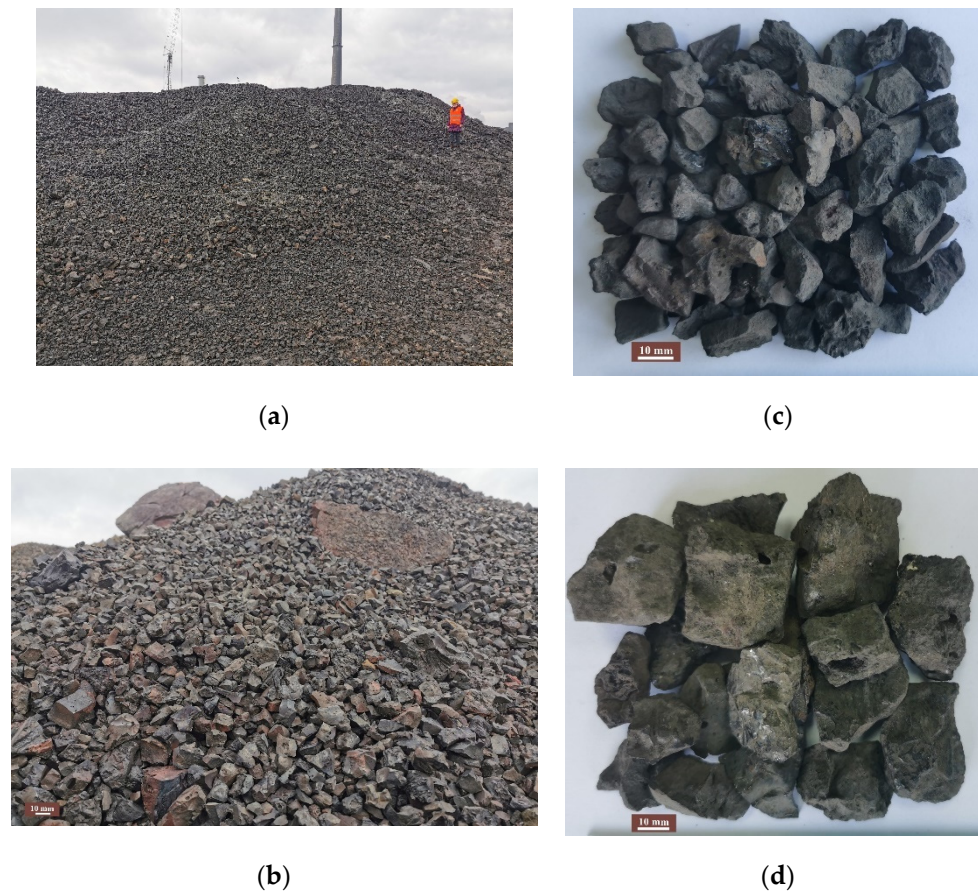

(**a**)

(**c**)

(**b**)

(**d**)

Figure 1. (**a**) Landfill of copper slag aggregates in the vicinity of the processing facilities of the Mining and Smelting Basin Bor; (**b**) macroscopic view of copper slag aggregate at the landfill; (**c**) macroscopic view of copper slag aggregate (8/16 mm); (**d**) macroscopic view of copper slag aggregate (16/31.5 mm).

The natural aggregate used in the research, which was obtained from the separation plant "New Separation", originally was acquired from the river Velika Morava near Paraćin (Serbia). Four standard fractions of this river aggregate (RA) were used in the study: 0/4 mm, 4/8 mm, 8/16 mm, and 16/31.5 mm. The particle-size distribution of the fractions used in the study is shown in Figure 2.

The mean particle sizes for cumulative percentages passing 50% ($d_{50\%}$) of river aggregate fractions 8/16 mm and 16/31.5 mm were 12.6 mm and 21.1 mm, respectively, while in the case of copper slag aggregate fractions, $d_{50\%}$ was 10.9 mm and 24.2 mm, respectively.

The cement used in the study for concrete preparation was blended Portland cement (PC), designated as CEM II/ A-L 42.5R, with a specific density of 3.15 mg/m^3. The cement was classified according to the European standard EN 197-1.

The chemical analyses of the copper slag aggregate were performed by different analytical methods: G—gravimetry; ICP-AES—inductively coupled plasma atomic emission spectroscopy; C—obtained by calculation; AAS—atomic absorption spectrophotometry; AES—atomic emission spectrophotometry; ACS—carbon and sulphur analyser; PHOT—photometry; SP—spectrophotometry; EG—electrogravimetry; V—volumetry; and A-Fe$_3$O$_4$—magnetite content analyser.
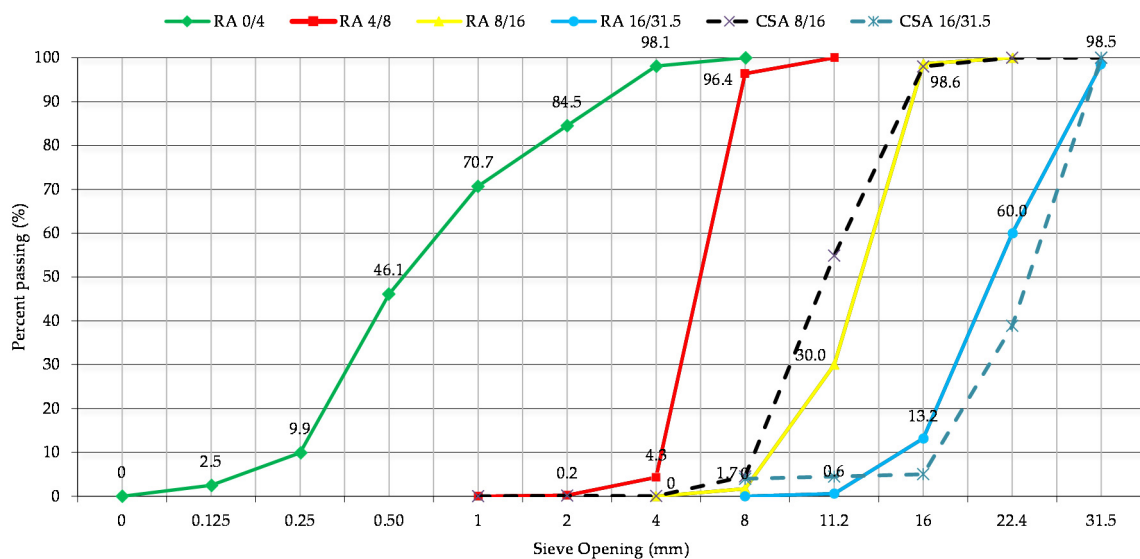
Figure 2. Particle-size distribution curves of river aggregate (RA) and copper slag aggregate (CSA).

A copper slag aggregate sample was mounted in epoxy resin, polished, and carbon-coated for SEM-EDS analysis. The analysis was performed using a JSM-IT300 (JEOL Ltd., Tokyo, Japan) coupled with an EDS AZtec Oxford Instruments XMax 50 mm^2 SDD energy-dispersive spectrometer, in high-vacuum mode, at an accelerating voltage of 20 kV and a probe current of ~0.1 nA. SEM images were acquired at a magnification of $1000\times$, according to the grain size of the analysed sample. Phase fractions (in vol%) were calculated using ImageJ software (v1.53a, National Institutes of Health, USA). The EDS elemental analysis was performed on all detected phases at multiple points. The internal standards were used for quantification, and all results were normalised to 100%. For homogenous crystalline phases, crystallochemical formulas were calculated based on the average composition.

Qualitative and quantitative assessment of the mineral composition of natural river aggregate was performed on 10/14 mm fraction according to EN 932-3.

The shape index of the previously prepared samples of both aggregates (CSA and RA) was determined according to EN 933-4, particle density and water absorption were determined according to EN 1097-6, and then a magnesium sulphate test was performed according to EN 1367-2. Resistance to fragmentation (Los Angeles test) was examined according to ASTM C 131, resistance to wear (M_{DE}) in a wet state was examined by a micro-Deval test according to EN 1097-1, and polished stone value (PSV) of the slag was determined according to EN 1097-8. The tests on the aggregates were performed in accordance with harmonized European standards (EN) and the American Society for Testing and Materials (ASTM) standard, which are shown in Figure 3. The categorization of the obtained test results was performed according to the EN 12620 standard for aggregates.

The testing of the physical and mechanical properties of three concrete mixtures, according to the standards shown in Figure 3, was performed as well. The first group consisted of control concrete specimens based on natural river aggregate; the concrete mixture in which 20% of 8/16 mm fraction and 50% of 16/31.5 mm fraction were substituted by volume (20% III + 50% IV) belonged in the second group; while in the third group, 50% of RA in both fractions 8/16 mm and 16/31.5 mm was replaced with corresponding fractions of CSA (50% III + 50% IV). Concrete mixes were prepared according to the recipe of the local concrete factory in order to facilitate the commercialization of concrete made with copper slag aggregate.
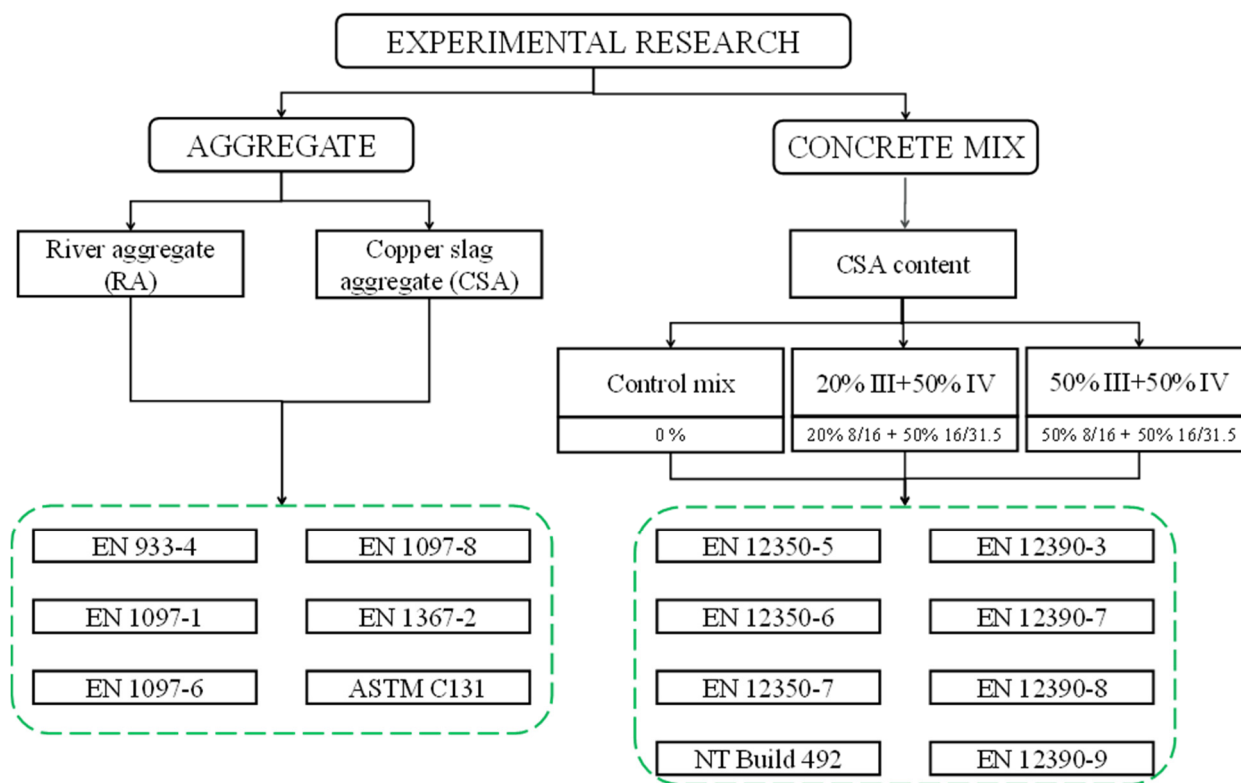
Figure 3. Diagram of testing methods for aggregates and concrete mixtures.

After the preparation of concrete mixtures and before casting into moulds, the consistency of fresh concrete (EN 12350-5), density (EN 12350-6), and air content (EN 12350-7) were determined. The density of hardened concrete (EN 12390-7) and compressive strength (EN 12390-3) were determined on 150 mm cubic samples. The compressive strength was examined after 1, 7, and 28 days of curing (EN 12390-2).

The test of water penetration under pressure was performed on 150 mm concrete cubes. The samples were tested after 28 days of curing, according to EN 12390-8. The samples were exposed to a constant water pressure of 5 bar for 72 h.

The resistance of concrete to chloride ion penetration was investigated on a (50 ± 2) mm section of a cast cylinder Ø100/H100 mm after 28 curing days, according to NT Build 492. The chloride ion migration through the concrete sample was performed with an electric current of 20 V for 24 h.

Samples in the shape of plates ($150 \times 150 \times 50$ mm) were cut out from 150 mm concrete cubes in order to test the freeze-thaw resistance of concrete in the presence of deicing salts. The test was performed after 28 curing days, according to EN 12390-9. The samples were subjected to cyclic freezing and thawing for 28 cycles. Visual assessment of the condition of the samples and measurements of the amount of chipped material was done after every 7 cycles.

3. Results

3.1. Chemical Analysis of Copper Slag Aggregate

Table 1 shows the chemical composition of the copper slag aggregate. It was determined that the slag predominantly consisted of silicon, iron, calcium, and aluminium oxides. The oxides of other elements were significantly less present. The copper content was below 0.50%.

Table 1. Chemical composition of copper slag aggregate (CSA).

Component	Content (%)	Analytical Method
SiO_2	42.06	G
Al_2O_3	3.53	ICP-AES
FeO	21.93	V
Fe_2O_3	6.84	C
Fe_3O_4	1.22	A-Fe_3O_4
CaO	20.06	AAS
MgO	0.50	AAS
SO_3	1.17	ACS
K_2O	0.43	AES
K	0.36	C
Na_2O	0.15	AES
Na	0.11	C
TiO_2	0.28	ICP-AES
Mn_2O_3	0.04	AAS
Cl-	0.01	PHOT/SP
Cu-ox	0.95	AAS
P_2O_5	0.09	ICP-AES
Cu	0.30	AAS/EG

Note: G—gravimetry; ICP-AES—inductively coupled plasma atomic emission spectroscopy; C—obtained by calculation; AAS—atomic absorption spectrometry; AES—atomic emission spectroscopy; ACS—carbon and sulphur analyser; PHOT—photometry; SP—spectrophotometry; EG—electrogravimetry; V—volumetry; and A-Fe_3O_4—magnetite content analyser.

3.2. Mineralogical Analysis of Copper Slag Aggregate

The SEM-EDS analysis revealed the presence of four general phases within the CSA (Figure 4). The absolutely dominant phase, comprising 82.35 vol% of the sample, was a silicate mineral of the clinopyroxene group, called hedenbergite (having the ideal formula $CaFeSi_2O_6$). With 13.94 vol%, it was followed by another silicate phase—devitrified glassy matrix. Two accessory phases were magnetite (an oxide mineral of the spinel group, having the ideal formula $FeFe_2O_4$) and sulphide droplets, comprising 2.34 and 1.37 vol% of the sample, respectively. Sulphide droplets were generally very heterogeneous, with Cu, Fe, and S as significant constituents. Their texture was very complex (Figure 5), due to a breakdown of solid solutions between chalcopyrite ($CuFeS_2$), bornite (Cu_5FeS_4), and digenite (Cu_9S_5). They also contained minute quantities of galena (PbS), sphalerite (ZnS), loellingite ($FeAs_2$), and other sulphide/arsenide minerals. Due to their complexity and low abundance, these sulphide droplets were considered as a single-phase in this paper.
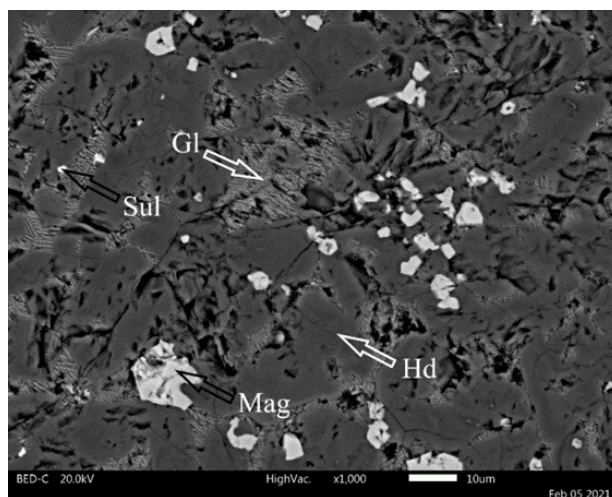

Figure 4. Backscattered electron image of sample CSA (abbreviations: Hd—hedenbergite; Mag—magnetite; Sul—sulphide droplets; Gl—galena).
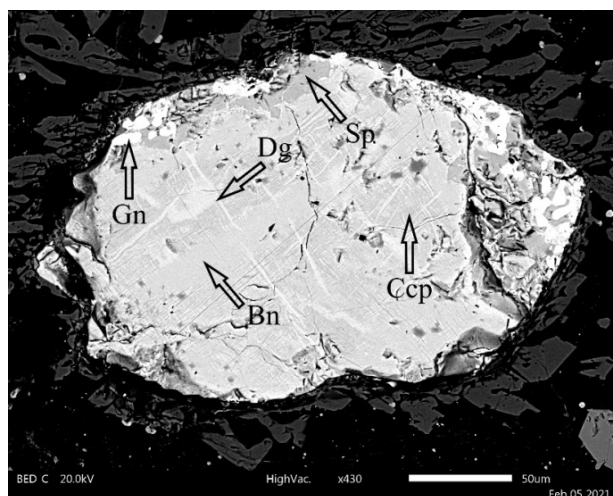
Figure 5. Backscattered electron image of a sulphide droplet (abbreviations: Ccp—chalcopyrite; Bn—bornite; Dg—digenite; Gn—galena; Sp—sphalerite).

The composition of all four phases detected in the CSA sample is given in Table 2, along with their abundances in vol%.

Table 2. Phase analysis of CSA using SEM-EDS.

Phase	Hedenbergite	Glassy Matrix	Magnetite	Sulphide Droplets
Element		wt%		
O	38.57	36.40	28.80	
Na		0.28		
Mg	0.58	0.02	0.06	
Al	1.56	4.18	1.27	
Si	21.18	17.93		
P		0.13		
S				32.89
K		0.90		
Ca	15.17	4.65	0.44	
Ti	0.13	0.19	1.16	
V			0.20	
Cr			0.02	
Mn	0.03	0.02		
Fe	22.73	33.31	67.98	19.50
Cu				47.61
Zn	0.05	0.09	0.07	
As		0.07		
Ba		1.83		
Σ	100.00	100.00	100.00	100.00
vol%	82.35	13.94	2.34	1.37
n *	10	8	4	7

* Number of measurement points.

Based on the values in Table 2, the crystallochemical formulas were calculated as follows:

$(Fe_{0.967}Zn_{0.002}Mg_{0.006}Ca_{0.025}Mn_{0.000})_{1.000}(Fe_{1.826}Al_{0.108}Ti_{0.056}Cr_{0.001}V_{0.009})_{2.000}O_{4.000}$ for magnetite and $(Ca_{0.942}Fe_{1.013}Mg_{0.059}Zn_{0.002}Mn_{0.001}Ti_{0.007}Al_{0.021})_{2.045}(Si_{1.877}Al_{0.123})_{2.000}O_{6.000}$ for hedenbergite.

Compared to the ideal formulas, both hedenbergite and magnetite showed enrichment in aluminium, with minor substitutions with magnesium, titanium, and other cations. Since the principal silicate crystal phase was hedenbergite, the glassy matrix remained very rich in iron. Having other minor elements distributed between crystal phases (hedenbergite, magnetite, and sulphides), it was enriched in aluminium and incompatible elements, such as barium, potassium, sodium, phosphorus, and arsenic.

3.3. Petrographic Analysis of River Aggregate

The petrographic analysis of gravel from the river Velika Morava, acquired from the separation plant "New Separation", is shown in Figure 6.
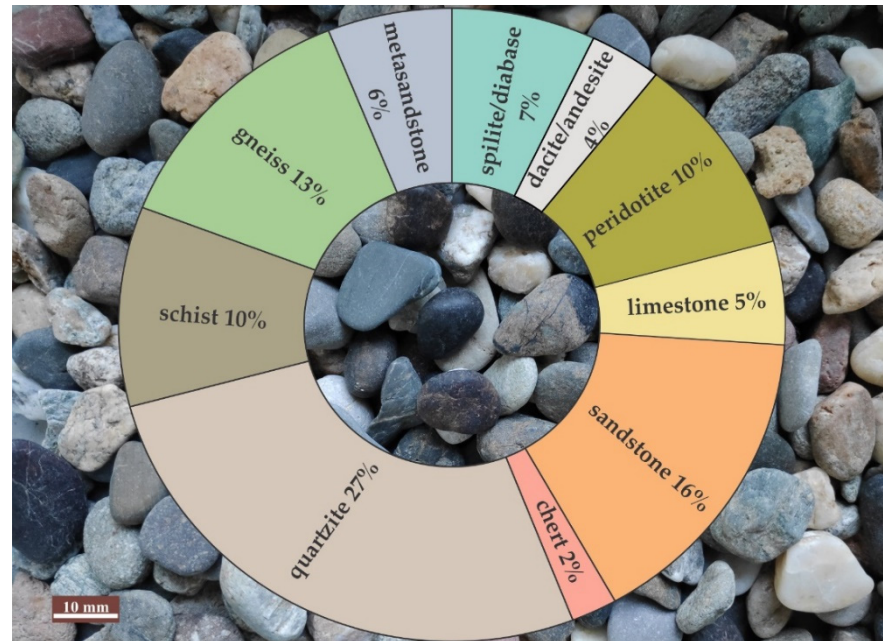

Figure 6. Chart of natural river aggregates (RA) shows different rock fragments in the 10/14 mm fraction. An image of the gravel used is in the background.

The 10/14 mm fraction consisted mostly of fragments of metamorphic rocks (56%) and the same quantity of sedimentary (23%) and igneous rocks (21%). Within the fragments of metamorphic rocks, the most represented were quartzites, then fragments of gneisses and schists. Among sedimentary rocks, sandstones were the most common, but a small number of limestones and cherts were also found. Igneous rocks formed fragments of spilite-diabase, dacite-andesites, and peridotites (often serpentinized) (Figure 6). The gravel fragments mostly had spherical and elongated shapes and smooth surfaces. No mineral grains were found in the tested fraction.

3.4. Geometric, Mechanical and Physical Characteristics of Aggregates

The particle size distribution of the RA and CSA fractions used in the study is shown in Figure 2. The percentage of undersized and oversized grains in the 8/16 mm fraction was 3.98% and 2.00%, respectively. For the 16/31.5 mm fraction, the percentage of undersized grains was 5.02%, while oversized grains were not detected.

The CSA grains were predominantly cubical and oblong with sharp edges, and their surface was smooth to glassy (Figure 1b). The average grain content with an unacceptable (flat) shape was low, amounting only to 5% (Table 3). The shape of natural aggregate grains was mostly oblong and cubical, and the grains had smooth, slightly rough, and sandy-rough surfaces due to the composition of rocks. In contrast, the average percentage of grain with an unfavourable shape was somewhat higher, at 16% (Table 3). The CSA was classified in the SI_{15} category and the RA in the SI_{20} category based on the geometric characteristics and grains with unfavourable shape content.

The value of the "Los Angeles" coefficient (LA 10) for the copper slag aggregate used in the study was almost three times better than the value obtained for the natural aggregate (LA 27). A similar conclusion was reached for resistance to wear: M_{DE} 4% for the CSA, compared to M_{DE} 10% for the natural aggregate (RA). The polished stone value for the CSA was 43. The results of the particle density test showed that the apparent particle density of CSA grains (3.33 mg/m^3) was higher than the particle density of natural aggregate

(2.58 mg/m^3). The CSA water-absorption percentage was two times lower than that of natural aggregate—0.6% and 1.2%, respectively. The magnesium sulphate test for salt-frost resistance showed that both aggregates were resistant to the effects of frost; i.e., they were classified in the highest category, MS$_{18}$ (Table 3).

Table 3. Physical and mechanical characteristics of aggregates.

Test Methods	Standard	Fraction (mm)	Determined Values		Categorised EN 12620	
			CSA	RA	CSA	RA
Shape index	EN 933-4	8/11	5		SI $_{15}$	
		10/14		16		SI $_{20}$
Resistance to fragmentation	SRPS B.B8.045 (ASTM C 131)	grading B	10	27	-	-
Resistance to wear	EN 1097-1	8/11	4		M$_{DE}$10	
		10/14		10		M$_{DE}$10
Polished stone value	EN 1097-8	standardized	43	-*	PSV$_{44}$	-
Particle density	EN 1097-6	8/11	ρ_a 3.40 ρ_{rd} 3.33 ρ_{ssd} 3.36		ρ_a 3.40 ρ_{rd} 3.33 ρ_{ssd} 3.36	
		10/14		ρ_a 2.66 ρ_{rd} 2.58 ρ_{ssd} 2.61		ρ_a 2.66 ρ_{rd} 2.58 ρ_{ssd} 2.61
Water absorption	EN 1097-6	8/11	0.6		WA$_{24}$ 1	
		10/14		1.2		WA$_{24}$ 2
Magnesium sulphate test	EN 1367-2	10/14	7	12	MS$_{18}$	MS$_{18}$

Note: CSA—copper slag aggregate; RA—river aggregate, SI—shape index 3:1 (%); LA—resistance to fragmentation (%); M$_{DE}$—resistance to wear (micro-Deval) in a wet state (%); PSV—polished stone value (coefficient); ρ_a—apparent particle density (mg/m^3); ρ_{rd}—oven-dried (real) particle density (mg/m^3); ρ_{ssd}—saturated and surface-dried particle density (mg/m^3); WA$_{24}$—water absorption of aggregate (%); MS—magnesium sulphate test (%). * Test was not performed because gravel was not used for wearing course (except for roads with low traffic loads and pedestrian and bike lanes).

3.5. Concrete Composition and Characteristics of Fresh Concrete

Three concrete mixtures with different content of recycled aggregate were prepared to examine the influence of CSA on the properties of fresh and hardened concrete. The particle size distribution of aggregates used for concrete mixtures is shown in Table 4.

Table 4. Particle size distribution of aggregates used for concrete mixtures

Mixture	Passing (%) through Sieve Opening (mm)										
	0.125	0.25	0.5	1	2	4	8	11.2	16	22.4	31.5
Control	1.0	4.0	18.4	28.3	33.8	39.9	54.8	61.2	78.0	90.0	99.6
20% III + 50% IV	1.0	4.0	18.4	28.3	33.8	39.9	55.4	62.6	77.0	87.4	99.8
50% III + 50% IV	1.0	4.0	18.4	28.3	33.8	39.9	55.6	64.1	76.9	87.4	99.8

Note: Control—control mixture; III—aggregate fraction 8/16 mm; IV—aggregate fraction 16/31.5 mm.

The concrete mix designs of all mixtures are presented in Table 5. The control concrete mixture was designed to meet the requirements for the C25/30 strength class, which is the most commonly used concrete strength class, with a 65% share [35]. The idea was to show that the CSA could be used in mixtures that were most common in practice. The mass of all components had constant values during the concrete design; only the second and third

mixture had coarse natural aggregate partially replaced with the CSA in vol%. This helped the assessment of the impact of the CSA on the behaviour of fresh and hardened concrete.

Table 5. Concrete mix design

Mixture	Water	River Aggregate (RA)				CSA Aggregate		Cement	W/CM *
	m_v	(0/4)	(4/8)	(8/16)	(16/31.5)	(8/16)	(16/31.5)	m_c	ω
	(kg/m^3)	(kg/m^3)	(kg/m^3)	(kg/m^3)	(kg/m^3)	(kg/m^3)	(kg/m^3)	(kg/m^3)	(–)
Control				343	428				
20% III + 50% IV	212	732	274	265	143	100	294	398	0.533
50% III + 50% IV				171	214	235	294		

* ratio of water to cementitious materials.

The results of tests on fresh concrete mixtures (consistency, density, and air content) are given in Table 6. Based on the obtained results, it can be concluded that the increase in CSA content increased the stiffness of fresh concrete. On the other hand, the mixtures with higher CSA content had higher densities and lower air content.

Table 6. Results of tests on fresh concrete mixtures.

Mixture	Flow Table Test (cm)	Density (kg/m^3)	Air Content (%)	Categorized EN 12350-5
Control	33.5	2331	1.9	F1
20% III + 50% IV	32.0	2431	1.7	F1
50% III + 50% IV	28.5	2443	1.7	F1

Note: Control—control mixture; III—aggregate fraction 8/16 mm; IV—aggregate fraction 16/31.5 mm.

3.6. Physical and Mechanical Characteristics of Hardened Concrete

The results showed that compressive strength was higher for mixtures with CSA than for the control mixture, regardless of the curing period (Table 7). For example, the compressive strength for the second (20% III + 50% IV) and third mixture (50% III + 50% IV) showed increases of 12.4% and 10.5%, respectively, after 28 curing days, compared to the control mixture. The same trend was observed in the case of the concrete density in the hardened state, which was higher by 5% and 7%, respectively.

Based on the obtained results, water penetration depth increased in mixtures with CSA (Table 7). Water absorption in the second (20% III + 50% IV) and third mixture (50% III + 50% IV) was higher by 55% and 28%, respectively, compared to the control mixture.

Table 7. Water penetration depth, compressive strength, and density of concrete.

Mixture	Average Water Penetration Depth (mm)	Compressive Strength (MPa)			Density (kg/m^3)
		After 1 Day	After 7 Days	After 28 Days	
Control	83	16.7	28.0	36.3	2303
20% III + 50% IV	129	20.1	34.1	40.8	2421
50% III + 50% IV	106	18.6	30.6	40.1	2462
Standard deviation		1.7	3.1	2.4	

Note: Control—control mixture; III—aggregate fraction 8/16 mm; IV—aggregate fraction 16/31.5 mm.

Resistance to chloride ion penetration was investigated on concrete samples prepared according to NT Build 492 standard. Based on the obtained values for chloride penetration depth, the effective chloride migration coefficient D_{RCM} was calculated [36]. These values are shown in Figure 7.
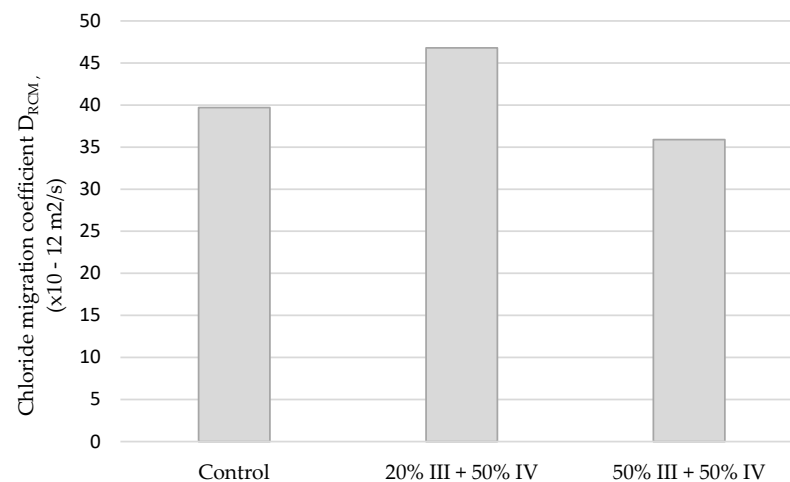
Figure 7. Results of resistance to chloride ion penetration.

The recorded effective chloride migration coefficient D_{RCM} for the control concrete showed a value of 39.7×10^{-12} cm^2/m, while for the second (20% III + 50% IV) and third mixtures (50% III + 50% IV), D_{RCM} was 46.8×10^{-12} cm^2/m and 36.0×10^{-12} cm^2/m, respectively.

Freeze-thaw resistance of concrete in the presence of de-icing salts was tested according to EN 12390-9. After 28 cycles, mass loss of 0.132 mg/mm^2 and 0.181 mg/mm^2 were measured on concrete samples from the control and second (20% III + 50% IV) mixture, respectively. The third concrete mixture (50% III + 50% IV) had a significantly higher mass loss of 0.596 mg/mm^2 (Figure 8). Visual examination of all concrete mixtures showed different degrees of degradation of the concrete surface (Figure 9). The concrete mixture (50% III + 50% IV) showed not only superficial damage of the fine material, but also plucking of the coarse aggregate grains (Figure 9c).
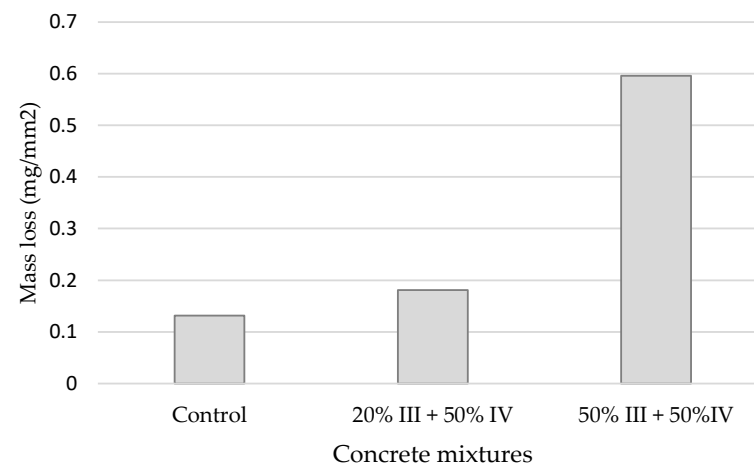

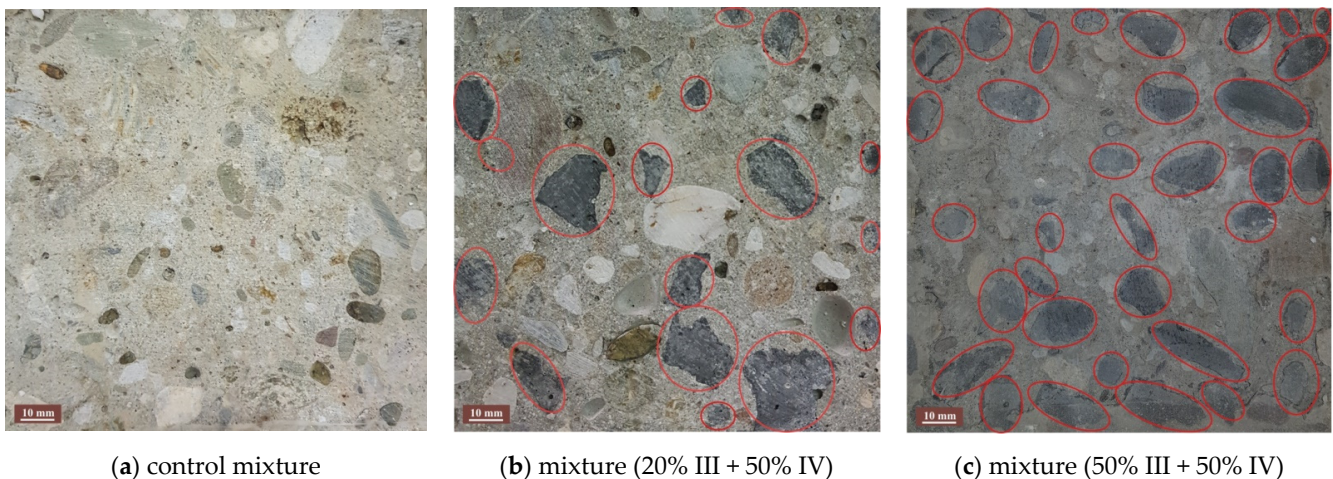**Figure 8.** Results of salt-frost resistance tests.

(**a**) control mixture   (**b**) mixture (20% III + 50% IV)   (**c**) mixture (50% III + 50% IV)

Figure 9. Concrete surface degradation after 28 cycles of freeze-thaw and salt exposure. Explanation: (**a**) visual examination of Control concrete mixture degradation; (**b**) visual examination of 20% III + 50% IV mixture degradation; (**c**) visual examination of 50% III + 50% IV mixture degradation. The positions of copper slag aggregate grains are highlighted by red circles.

4. Discussion

The properties of copper slag aggregate and natural river aggregate used for concrete preparation were investigated in this study. The coarse natural RA was partially replaced (20% and 50% by volume) with CSA. Moreover, the experiments included testing of properties of concrete mixtures prepared with both types of aggregate.

The copper slag did not have a uniform chemical composition. Some researchers found that the content of chemical compounds in slag varied (Fe_2O_3: 35–60%, SiO_2: 25–40%, CaO: 2–10%, Al_2O_3: 3–15%, CuO: 0.3–2.1%, MgO: 0.7–3.5%) [20]. Other researchers suggested that the content of CaO and MgO could be higher (28% and 12%, respectively) [13,37].

The chemical analysis of copper slag sampled from landfills in the vicinity of processing facilities in Bor at different periods revealed two similar data groups. The first group of analysed slag had a lower content of silicon and calcium and higher content of iron [34,38–40]. The second group of samples had a higher content of silicon and calcium and a lower content of iron [31]. The slag used in this research was taken from the second group.

Nonferrous slags, such as copper slag, can be classified either as basic, acid, or neutral, based on the silicate degree and ratio of basic and acid oxides. The silicate degree and ratio of basic and acid oxides [41] can be calculated as:

$$\text{Silicate degree} = \frac{\text{moles of acid oxygen from } SiO_2}{\text{moles if basic oxygen from CaO, MgO, FeO}} \tag{1}$$

$$\frac{MO}{SiO_2}, \text{ where MO is basic oxides} \tag{2}$$

Based on these formulas, the silicate degree for this pyroxene copper slag was 2.1, and the ratio of basic oxides and silicon oxide was 1. According to the proposed categorization (Table 8), the tested slag belonged to the group of acid slags.

Table 8. Classification of nonferrous slags.

	Silicate Degree	MO/SiO$_2$	Slag
Classification	<1	>2	basic
	>1	<2	acid
	2	2	neutral
2020 (pyroxene copper slag)	2.1	1	acid

Note: MO—basic oxides.

This can also be confirmed by the three-component diagram [42] for CaO–SiO$_2$–Al$_2$O$_3$ (Figure 10). Fayalite and magnetite were the most abundant minerals in the copper slag aggregates, with an average CaO content of 5% and Fe$_2$O$_3$ content of 45% [43]. The increased content of calcium and silicon in the chemical analysis in this study (CaO 20%; S$_i$O$_2$ 42%) affected the increased content of minerals from the clinopyroxene group (hedenbergite, 82.35%), which was confirmed by SEM analysis. The remaining calcium and silicon content were bound to the silicate phase—devitrified glassy matrix (13.94%), and iron was predominantly bound to the oxide mineral from spinel group—magnetite and sulphide droplets with a content of 2.34% and 1.37%, respectively (Table 2).

Petrographic analysis of the natural aggregate used in the concrete mixture showed that 95% of gravel consisted of silicate rocks, i.e., quartzites, gneisses, schists, sandstones, cherts, spilite-diabase, dacite-andesites, and peridotites fragments. The content of the limestone was low (5%).

It is known that the granulated slag obtained during the pyrometallurgical process of copper smelting has spherical grains with sharp edges and mostly consists of oxide and several sulphide minerals [44]. The aggregate grain shape depends on the technology used for copper production and the method of crystallisation of copper slag at the landfill [20]. The landfill from which the slag was taken in Bor also had grains of a favourable shape (SI 5). This property of the aggregate had a positive effect on the compactness of the aggregate in the concrete mixtures and the compressive strength of the hardened concrete. The gravel's grain shape was somewhat unfavourable due to the presence of slate and gneiss (23%) (SI 16).
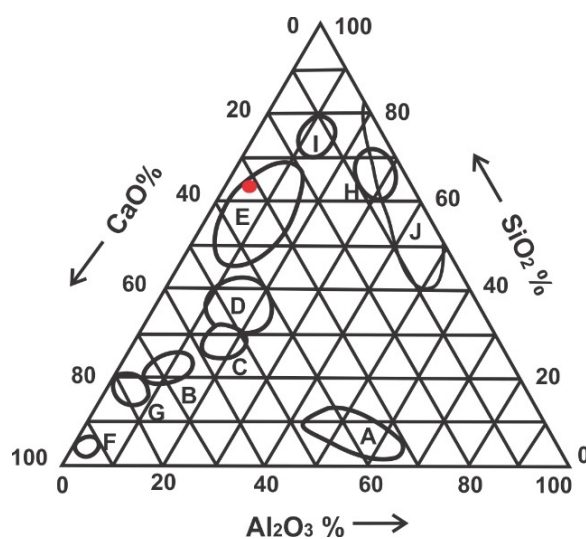

Figure 10. Position of the investigated slag (red dot) in the ternary diagram of binders and additives zones [42]. Note: A—aluminous cement; B—Portland cement; C—cement with slag; D—basic slag; E—acid slag; F—quicklime; G—hydrated lime; H—trass (pozzolan); I—silicate substances; J—pozzolans (natural and artificial).

The resistance to fragmentation of the CSA was more favourable compared to the RA. The obtained values for resistance to fragmentation of the CSA and RA were LA 10% and 26%, respectively. This means that the CSA grains were almost three times more resistant to fragmentation than the RA grains. The results of the micro-Deval test on resistance to wear for the CSA and RA samples were M_{DE} 4% and 10%, respectively. The obtained values indicated better resistance to wear for the CSA samples. This confirmed that granulated copper slag had favourable technical properties such as strength and resistance to wear [45].

The polished stone value of CSA was PSV 43. The obtained value was in accordance with the visual perception of a strong, compact aggregate with fine-grained, smooth to glassy grain surfaces (Figure 1b). The polished stone value of this type of slag was lower than the determined value for steel slag (PSV 54); however, it was higher than the value determined for limestone (PSV 34, 37) [46].

The particle-density tests results showed that the actual particle density of the CSA was 3.33 mg/m^3, which was 22.5% higher compared to the RA (2.58 mg/m^3). However, water absorption of the CSA was two times lower than water absorption of the RA (0.6% and 1.2%, respectively). The investigated aggregates' properties indicated that the concrete mixture with a higher copper slag aggregate content had higher values of density than the control mixture, both in fresh and hardened states.

Some researchers determined that the values of water absorption and particle density also depended on the method of crystallization of copper slag at the landfill. Amorphous structures created by adding water during the cooling process had higher water absorption and lower particle density than those cooled in the air due to a more porous texture [20]. The internal structure of the granulated copper slag was glassy [47]. Compared to the above-mentioned slag, the slag from the landfill at RTB Bor was cooled in air, without water, and therefore it had a higher particle density and lower water absorption. The slag's cavities were sporadically present (Figure 1c, d); however, they had micrometre dimensions and did not retain water, which was determined by lower water absorption of the copper slag aggregate (CSA) compared to the natural aggregate (NA).

Both investigated aggregates were resistant to frost and belonged to the MS_{18} category. However, the copper slag was more resistant to frost (MS 7) than the river gravel (MS 12) because the presence of slate and peridotite reduced its frost resistance.

The increase of CSA content in concrete mixtures resulted in stiffer consistency compared to the control mixture. This occurred because the CSA grains had a larger specific surface and less mobility. The CSA grains were rougher and had sharper edges than the RA grains, which caused greater friction between the grains. The amount of used CSA did not have a significant effect on entrained air content in the fresh concrete mixtures.

The densities of fresh concrete from the second (20% III + 50% IV) and the third group (50% III + 50% IV) were higher by 4% and 5%, respectively, compared to the control mixture. The hardened concrete densities from the second (20% III + 50% IV) and the third group (50% III + 50% IV) were higher by 5% and 7%, respectively, compared to the control mixture. This occurred due to the higher particle density of the CSA compared to the RA. Based on the flow-table test, the tested concrete mixtures were categorized as class F1. Concrete mixtures from the second (20% III + 50% IV) and third (50% III + 50% IV) groups had higher compressive strength by 12.4% and 10.5%, respectively, after 28 days of curing. The higher compressive strength of the CSA grains and better interaction between them due to their roughness and sharp edges caused the increase in the mixtures' compressive strengths. The standard deviations for compressive strength of control mixture and concrete mixtures from the second and third group after 1, 7, and 28 days of curing amounted to 1.7, 3.1, and 2.4, respectively.

The water-penetration resistance of concrete from the second (20% III + 50% IV) and third (50% III + 50% IV) groups were lower by 55.4% and 27.7%, respectively, compared to the control mixture. At first, this did not seem logical since the CSA grains had lower water absorption than the RA. However, the water-penetration resistance of concrete largely depends on the concrete mixture's compactness, i.e., the presence of capillary pores

in the cement matrix. The increase in pore density caused a decrease in the concrete's water-penetration resistance. Considering that during the preparation of all three concrete mixtures, the content of cement and water remained unchanged due to lower water absorption of the CSA grains, the content of free water increased in the second (20% III + 50% IV) and third (50% III + 50% IV) mixtures. Thus, the increase of free water in the concrete mixtures directly affected the increase of volume of capillary pores in the concrete structure.

There were no significant changes in chloride ion penetration resistance, quantified by the chloride migration coefficient (D_{RCM}), in all three concrete mixtures. The analysis of the obtained results for the control mixture and concrete with CSA replacement showed that the D_{RCM} value was higher than 16×10^{-12}; therefore, this concrete could be suitable for use in clean environments without aggressive influences [48,49]. However, the main cause for higher chloride migration through concrete, as well as for increased water penetration, was the higher porosity of the cement matrix.

In addition, the higher porosity of the cement matrix in the mixtures with the CSA caused intensified degradation of the concrete surface due to the combined effect of the freeze-thaw and de-icing salts. This is noticeable in the images of concrete surfaces after 28 cycles of freezing and thawing (Figure 9), especially for the third (50% III + 50% IV) group of concrete samples. However, the material's evident scaling during the investigation was expected to some extent, since the tested mixture was not initially designed to be resistant to this influence.

From the aspect of concrete durability (water-penetration resistance, resistance to chloride ion penetration, and salt-frost resistance), the mixtures prepared with partial replacement of RA with CSA had lower durability than the control mixture. The general cause of this was the higher porosity of the cement matrix due to a greater amount of free water. The solution for this problem would be simple: the amount of added water in the mixtures prepared with the CSA should be reduced. As in the case of the control mixture, the same concrete workability could be achieved by adding a small amount of chemical admixture–plasticiser.

5. Conclusions

The experiments presented in this paper included investigations of chemical, mineralogical-petrographic, and physical-mechanical properties of copper slag aggregates and natural river aggregate, as well as physical-mechanical properties of concrete mixtures prepared with partial replacement of coarse river aggregate (RA) with copper slag aggregate (CSA). The investigation was performed with the aim to compare the behaviour of standard concrete made with RA and concrete made with CSA as an innovative solution for the use of this by-product. The conclusions based on the obtained test results are the following:

- Copper slag from RTB Bor is a mineral material with predominant silicon, calcium, iron, and aluminium oxides, while copper content did not exceed 1%;
- The slag consisted of the following minerals: silicate mineral of the clinopyroxene group and devitrified glassy matrix. Two accessory phases were magnetite and sulphide droplets;
- River aggregate consisted mostly of fragments of metamorphic rocks and the same quantity of sedimentary and igneous rocks;
- Compared to RA, CSA had better resistance to fragmentation and wear, higher particle density, and lower water absorption. These characteristics are in accordance with the European technical requirements for aggregates used in concrete;
- The increase of CSA content increased concrete density, both in the fresh and hardened states;
- The replacement of RA fractions 8/16 mm and 16/31.5 mm with CSA aggregate in the amount of 20 + 50% and 50 + 50% by volume led to increases in compressive strength by 12.4% and 10.5%, respectively;

- Lower water absorption of the CSA compared to the RA, with an unchanged amount of cement and water, caused an increase in the porosity of the cement matrix;
- Increased cement-matrix porosity resulted in reduced water penetration resistance and salt-frost resistance in concrete mixtures with CSA;
- The resistance to chloride ion penetration of the CSA mixtures was not significantly changed compared to the control mixture.

In order to increase the durability of concrete made with CSA, the amount of water used for mixture preparation should be reduced because of the lower water absorption of CSA. This way, the effective amount of water could stay constant, which would increase the overall durability of concrete.

Author Contributions: Conceptualization, D.Z.; methodology, formal analysis, investigation, resources and data curation, S.F., O.Đ., and A.R.; writing—original draft preparation, S.F.; writing—review and editing, O.Đ., A.R., and D.Z.; visualization, S.F. and O.Đ.; supervision, A.R. and D.Z.; project administration, D.Z. and S.F.; funding acquisition, S.F. All authors have read and agreed to the published version of the manuscript.

Data Availability Statement: The data presented in this study are available on request from the corresponding author.

Conflicts of Interest: The authors declare no conflict of interest.

References

1. Tam, C.; Taylor, M.; Gielen, D.; Twigg, C.; Klee, H.; Rocha, P.; Meer, R. *Cement Technology Roadmap 2009—Carbon Emissions Reductions up to 2050*; World Business Council for Sustainable Development: Geneva, Switzerland, 2009.
2. Zhao, Q.; Liu, X.; Jiang, J. Effect of curing temperature on creep behavior of fly ash concrete. *Constr. Build. Mater.* **2015**, *96*, 326–333. [CrossRef]
3. Al-Jabri, K.S.; Hisada, M.; Al-Saidy, A.H.; Al-Oraimi, S.K. Performance of high strength concrete made with copper slag as a fine aggregate. *Constr. Build. Mater.* **2009**, *23*, 2132–2140. [CrossRef]
4. Sankh, A.C.; Biradar, P.M.; Naghathan, S.J.; Ishwargol, M.B. Recent Trends in Replacement of Natural Sand with Different Alternatives Akshay. *IOSR J. Mech. Civ. Eng. (IOSR-JMCE)* **2002**, *12*, 180–183.
5. De Leeuw, J.; Shankman, D.; Wu, G.; de Boer, W.F.; Burnham, J.; He, Q.; Yesou, H.; Xiao, J. Strategic assessment of the magnitude and impacts of sand mining in Poyang Lake, China. *Reg. Environ. Chang.* **2010**, *10*, 95–102. [CrossRef]
6. Kuntikana, G.; Singh, D.N. Contemporary Issues Related to Utilization of Industrial Byproducts. *Adv. Civ. Eng. Mater.* **2017**, *6*, 20160050. [CrossRef]
7. Maharishi, A.; Singh, S.P.; Gupta, L.K. Shehnazdeep Strength and durability studies on slag cement concrete made with copper slag as fine aggregates. *Mater. Today Proc.* **2020**. [CrossRef]
8. Prasad, P.S.; Ramana, G.V. Feasibility study of copper slag as a structural fill in reinforced soil structures. *Geotext. Geomembr.* **2016**, *44*, 623–640. [CrossRef]
9. Alter, H. The composition and environmental hazard of copper slags in the context of the Basel Convention. *Resour. Conserv. Recycl.* **2005**, *43*, 353–360. [CrossRef]
10. Sharma, R.; Khan, R.A. Sustainable use of copper slag in self compacting concrete containing supplementary cementitious materials. *J. Clean. Prod.* **2017**, *151*, 179–192. [CrossRef]
11. Baghalha, M.; Papangelakis, V.G.; Curlook, W. Factors affecting the leachability of Ni/Co/Cu slags at high temperature. *Hydrometallurgy* **2007**, *85*, 42–52. [CrossRef]
12. Zivkovic, Z.; Mitevska, N.; Mihajlovic, I.; Nikolic, D. The influence of the silicate slag composition on copper losses during smelting of the sulfide concentrates. *J. Min. Metall. Sect. B Metall.* **2009**, *45*, 23–34. [CrossRef]
13. Wang, D.; Wang, Q.; Huang, Z. Reuse of copper slag as a supplementary cementitious material: Reactivity and safety. *Resour. Conserv. Recycl.* **2020**, *162*, 105037. [CrossRef]

14. Dhir, R.K.; de Brito, J.; Mangabhai, R.; Lye, C.Q. Use of Copper Slag in Geotechnical Applications. In *Sustainable Construction Materials: Copper Slag*; Elsevier: Amsterdam, The Netherlands, 2017; pp. 211–245.

15. Dimitrijevic, M.; Urosevic, D.; Milic, S.; Sokic, M.; Markovic, R. Dissolution of copper from smelting slag by leaching in chloride media. *J. Min. Metall. Sect. B Metall.* **2017**, *53*, 407–412. [CrossRef]

16. Sharma, R.; Khan, R.A. Durability assessment of self compacting concrete incorporating copper slag as fine aggregates. *Constr. Build. Mater.* **2017**, *155*, 617–629. [CrossRef]

17. Dey, A.; Dev, D.; Saha, P. Use of copper slag as sustainable aggregate. *Icsci 2014* **2015**, *1*, 229–240.

18. Khanzadi, M.; Behnood, A. Mechanical properties of high-strength concrete incorporating copper slag as coarse aggregate. *Constr. Build. Mater.* **2009**, *23*, 2183–2188. [CrossRef]

19. Al-Jabri, K.S.; Al-Saidy, A.H.; Taha, R. Effect of copper slag as a fine aggregate on the properties of cement mortars and concrete. *Constr. Build. Mater.* **2011**, *25*, 933–938. [CrossRef]

20. Shi, C.; Meyer, C.; Behnood, A. Utilization of copper slag in cement and concrete. *Resour. Conserv. Recycl.* **2008**, *52*, 1115–1120. [CrossRef]

21. Neves, R.; Branco, F.; de Brito, J. Field assessment of the relationship between natural and accelerated concrete carbonation resistance. *Cem. Concr. Compos.* **2013**, *41*, 9–15. [CrossRef]

22. Gorai, B.; Jana, R.K. Premchand Characteristics and utilisation of copper slag—A review. *Resour. Conserv. Recycl.* **2003**, *39*, 299–313. [CrossRef]

23. Shi, C.; Qian, J. High performance cementing materials from industrial slags—A review. *Resour. Conserv. Recycl.* **2000**, *29*, 195–207. [CrossRef]

24. Mavroulidou, M. Mechanical Properties and Durability of Concrete with Water Cooled Copper Slag Aggregate. *Waste Biomass Valorization* **2017**, *8*, 1841–1854. [CrossRef]

25. Lori, A.R.; Hassani, A.; Sedghi, R. Investigating the mechanical and hydraulic characteristics of pervious concrete containing copper slag as coarse aggregate. *Constr. Build. Mater.* **2019**, *197*, 130–142. [CrossRef]

26. Ibrahim, H.A.; Abdul Razak, H. Effect of palm oil clinker incorporation on properties of pervious concrete. *Constr. Build. Mater.* **2016**, *115*, 70–77. [CrossRef]

27. Zarauskas, L.; Skripkiūnas, G.; Girskas, G. Influence of Aggregate Granulometry on Air Content in Concrete Mixture and Freezing—Thawing Resistance of Concrete. *Procedia Eng.* **2017**, *172*, 1278–1285. [CrossRef]

28. Aligizaki, K.K. *Pore Structure of Cement-Based Materials*; CRC Press: Boca Raton, FL, USA, 2005; ISBN 9780429079313.

29. Yeih, W.; Fu, T.C.; Chang, J.J.; Huang, R. Properties of pervious concrete made with air-cooling electric arc furnace slag as aggregates. *Constr. Build. Mater.* **2015**, *93*, 737–745. [CrossRef]

30. Zhang, Z.; Zhang, Y.; Yan, C.; Liu, Y. Influence of crushing index on properties of recycled aggregates pervious concrete. *Constr. Build. Mater.* **2017**, *135*, 112–118. [CrossRef]

31. Cadjenovic, B.; Marjanovic, V.; Ljubojev, V.; Milanovic, D. Possibilities of use the copper matte from smelter slag in its direct bakrenca of smelting slag in its direct discharge from furnace. *Min. Eng.* **2012**, 143–148. [CrossRef]

32. Đorđević, J.; Orešković, M.; Mladenović, G. The possibility of the application of copper slag in asphalt mixtures. *J. Road Traffic Eng.* **2018**, *64*. [CrossRef]

33. Maluckov, B. Waste from mining-metallurgical production of copper and treatment of it. *Tehnika* **2017**, *72*, 819–824. [CrossRef]

34. Stanojlović, R.; Štirbanović, Z.; Sokolović, J. New technological procedure for sustainable processing of mining technological waste. *Min. Eng.* **2012**, *1*, 75–88. [CrossRef]

35. Jevtic, D.; Zakic, D.; Savic, A.; Radevic, A. Statistical analysis of concrete quality testing results. *Build. Mater. Struct.* **2014**, *57*, 45–52. [CrossRef]

36. Castellote, M.; Andrade, C.; Alonso, C. Measurement of the steady and non-steady-state chloride diffusion coefficients in a migration test by means of monitoring the conductivity in the anolyte chamber. Comparison with natural diffusion tests. *Cem. Concr. Res.* **2001**, *31*, 1411–1420. [CrossRef]

37. Killick, D.; Miller, D.; Thondhlana, T.P.; Martinón-Torres, M. Copper mining and smelting technology in the northern Lowveld, South Africa, ca. 1000 CE to ca. 1880 CE. *J. Archaeol. Sci.* **2016**, *75*, 10–26. [CrossRef]

38. Marinković, L. *Contribution to Investigations on the Possibility of Copper Blast Furnace Slag from Bor Usage in Pavements Construction*; The University of Belgrade, Faculty of Civil Engineering: Belgrade, Serbia, 1989.

39. Gržetić, I.; Brčeski, I. Degradation of Bor slags as the contamination process. In Proceedings of the Naša ekološka istina '95, Hotel "Jezero", Borsko jezero, Bor, Serbia, 31 May–2 June 1995; pp. 95–100.

40. Urošević, D. *Copper Extraction from Smelting Slag by Combined Methods*; University of Belgrade, Technical faculty in Bor: Belgrade, Serbia, 2016.

41. Ray, H.S.; Sridhar, R.; Abraham, K.P. *Extraction of Nonferrous Metals*; EWP: New Delhi, India, 2014; ISBN 8185095639.

42. Brzaković, P. Prilog problemu sistematizacije veziva na bazi cementnog klinkera i dodataka nemetaličnog porekla. *Građevinski Mater. Konstr.* **2002**, *45*, 23–33.

43. Dhir Obe, R.K.; de Brito, J.; Mangabhai, R.; Lye, C.Q. *Sustainable Construction Materials: Copper Slag*; Woodhead Publishing: London, UK, 2016; ISBN 9780081009864.

44. Ljubojev, V.; Marjanovic, V.; Milanovic, D.; Stankovic, S. Mineralogical characteristics of slag (from the Flotation plant of RTB Bor) granulated in the laboratory conditions. *Min. Metall. Eng. Bor.* **2015**, 1–12. [CrossRef]

45. Moosberg, H.; Lagerblad, B.; Forssberg, E. The use of by-products from metallurgical and mineral industries as filler in cement-based materials. *Waste Manag. Res.* **2003**, *21*, 29–37. [CrossRef]
46. Crisman, B.; Ossich, G.; Bevilacqua, P.; Roberti, R. Degradation prediction model for friction of road pavements with natural aggregates and steel slags. *Appl. Sci.* **2020**, *10*, 32. [CrossRef]
47. Feng, Y.; Yang, Q.; Chen, Q.; Kero, J.; Andersson, A.; Ahmed, H.; Engström, F.; Samuelsson, C. Characterization and evaluation of the pozzolanic activity of granulated copper slag modified with CaO. *J. Clean. Prod.* **2019**, *232*, 1112–1120. [CrossRef]
48. Yuan, Q.; Santhanam, M. Erratum to: Test Methods for Chloride Transport in Concrete. In *Performance of Cement-Based Materials in Aggressive Aqueous Environments*; Springer: Dordrecht, The Netherlands, 2013; p. E1.
49. Ugur, I.; Demirdag, S.; Yavuz, H. Effect of rock properties on the Los Angeles abrasion and impact test characteristics of the aggregates. *Mater. Charact.* **2010**, *61*, 90–96. [CrossRef]